M.Sc. Physics

Sudeb Sarkar

2021

PHOTONIC CRYSTALS

A DISSERTATION

SUBMITTED IN PARTIAL FULFILLMENT OF THE REQUIREMENTS
FOR THE AWARD OF THE DEGREE
OF

MASTER OF SCIENCE
IN
PHYSICS

Submitted by:

SUDEB SARKAR

2K19/MSCPHY/01

Under the supervision of

Prof R.K. Sinha

DEPARTMENT OF APPLIED PHYSICS
DELHI TECHNOLOGICAL UNIVERSITY
(Formerly Delhi College of Engineering)
Bawana Road, Delhi-110042

MAY, 2021

CANDIDATE'S DECLARATION

I, Sudeb Sarkar, Roll No 2K19/MSCPHY/01 student of M.Sc. Physics, hereby declare that the project Dissertation titled "Photonic Crystals" which is submitted by me to the Department of Applied Physics, Delhi Technological University, Delhi in partial fulfillment of the requirement for the award of the degree of Master of Science, is original and not copied from any source without proper citation. This work has not previously formed the basis for the award of any Degree, Diploma Associateship, Fellowship or other similar title or recognition.

Place: Delhi
Date: 30 May 2021

Name of Student:
Sudeb Sarkar

ACKNOWLEDGEMENT

I'd like to thank Prof. R.K. Sinha, TIFAC-Centre of Relevance and Excellence in Fiber Optics and Optical Communication, Department of Applied Physics, Delhi Technological University for giving me this topic to research, and Delhi Technological University for giving me the opportunity to pursue this research project.
I'd like to thank my mother Mrs. Bashori Sarkar for all the support she's given me throughout the course of this project.

CERTIFICATE

I hereby certify that the Project Dissertation titled "Photonic Crystals" which is submitted by Sudeb Sarkar, Roll No 2K19/MSCPHY/01 Department of Applied Physics, Delhi Technological University, Delhi in partial fulfillment of the requirement for the award of the degree of Master of Science, is a record of the project work carried out by the student under my supervision. To the best of my knowledge this work has not been submitted in part or full for any Degree or Diploma to this University or elsewhere.

Place: Delhi
Date: 30 May 2021

(Prof. R.K. Sinha)
SUPERVISOR

PLAGIARISM REPORT

turnitin

thesis for plagiarism check.pdf
May 31, 2021
6290 words / 28883 characters

thesis for plagiarism check.pdf

Sources Overview

7%
OVERALL SIMILARITY

1	doaj.org INTERNET	<1%
2	Sheffield Hallam University on 2020-09-18 SUBMITTED WORKS	<1%
3	www.emnc.org INTERNET	<1%
4	elpub.bib.uni-wuppertal.de INTERNET	<1%
5	epdf.pub INTERNET	<1%
6	Botten, Lindsay, Ross McPhedran, Martijn de Sterke, Nicolaei Nicorovic, Ara Asatryan, Geoffrey Smith, Timothy Langtry, Thomas White... CROSSREF	<1%
7	Min Qiu, Sailing He. "FDTD algorithm for computing the off-plane band structure in a two-dimensional photonic crystal with dielectric ... CROSSREF	<1%
8	Natalia Malkova. "Tunable resonant light propagation through 90° bend waveguide based on strained photonic crystal", Journal of Phy... CROSSREF	<1%
9	Z. C. He, J. Y. Hu, Eric Li. "An uncertainty model of acoustic metamaterials with random parameters", Computational Mechanics, 2018 CROSSREF	<1%
10	Dong-Ho Lee, June Gyu Park, Hong Seung Kim, Ji Yong Bae et al. "Effect of higher-order diffraction on the interference formed by Brag... CROSSREF	<1%
11	Xiao Wang, Haitao Jiang, Yuan Li, Chao Yan, Fusheng Deng, Yong Sun, Yunhui Li, Yunlong Shi, Hong Chen. "Transport properties of dis... CROSSREF	<1%
12	citeseerx.ist.psu.edu INTERNET	<1%
13	Fisher, . "Lattice Structure, Phonons, and Electrons", Thermal Energy at the Nanoscale, 2013. CROSSREF	<1%
14	Indian Institute of Technology Guwahati on 2015-05-16 SUBMITTED WORKS	<1%
15	Kazuhiko Ogusu, Kosuke Takayama. "Transmission characteristics of photonic crystal waveguides with stubs and their application to ... CROSSREF	<1%
16	Keshav Samrat Modi, Satya Pratap Singh, Jasleen Kaur, Umesh Tiwari, Ravindra Kumar Sinha. "All dielectric metasurface based tunabl... CROSSREF	<1%
17	dyuthi.cusat.ac.in INTERNET	<1%

18	Jong Wook Noh. "In-plane photonic transduction of silicon-on-insulator microcantilevers", Optics Express, 08/04/2008 CROSSREF	<1%
19	La Trobe University on 2020-05-07 SUBMITTED WORKS	<1%
20	University of Sydney on 2021-05-14 SUBMITTED WORKS	<1%
21	arizona.openrepository.com INTERNET	<1%
22	documents.mx INTERNET	<1%
23	Imperial College of Science, Technology and Medicine on 2018-04-30 SUBMITTED WORKS	<1%
24	Nishant Shankhwar, Ravindra Kumar Sinha. "Zero Index Metamaterials", Springer Science and Business Media LLC, 2021 CROSSREF	<1%
25	University of Nottingham on 2017-02-02 SUBMITTED WORKS	<1%

Excluded search repositories:

- None

Excluded from Similarity Report:

- Bibliography
- Quotes
- Small Matches (less than 10 words).

Excluded sources:

- None

ACCEPTANCE LETTER

SOCIETY FOR EDUCATION

International Conference on Physics (ICOP-21)

11TH JULY 2021, VARANASI, India

Acceptance Letter

Event Link : https://www.sfe.net.in/conf/index.php?id=1467238

Paper Id: SFE_45876

Paper Title: Effect of geometries on photonic bandgaps.

Authors: Sudeb Sarkar, Prof. R.K. Sinha,

Dear Researchers,

With heartiest congratulations I am pleased to inform you that based on the recommendations of the reviewers and the Technical Program Committees, your paper identified above has been accepted for publication and oral presentation by **International Conference on Physics (ICOP-21).**

(ICOP-21) conference received over 80 submissions from countries and regions, reviewed by international experts and your paper cleared all the criteria, got accepted for the conference. Your paper will be published in the conference proceeding and UGC approved journal after registration.

For registration : https://www.sfe.net.in/conf/registration.php?id=1467238

Herewith, the conference committee sincerely invites you to come to present your paper at **ICOP-21** to be held on **11TH JULY 2021 at VARANASI**.

Sincerely,

Dr. James Crusoe
President
Society For Education (SFE)

DOI Directory .com Identifying Articles

ResearchPEDIA .org

DRJI

UGC University Grants Commission

+91-9677007228

info@sfe.net.in

www.sfe.net.in

INDEXING EVIDENCE

CONFERENCE PARTICIPATION PAYMENT PROOF

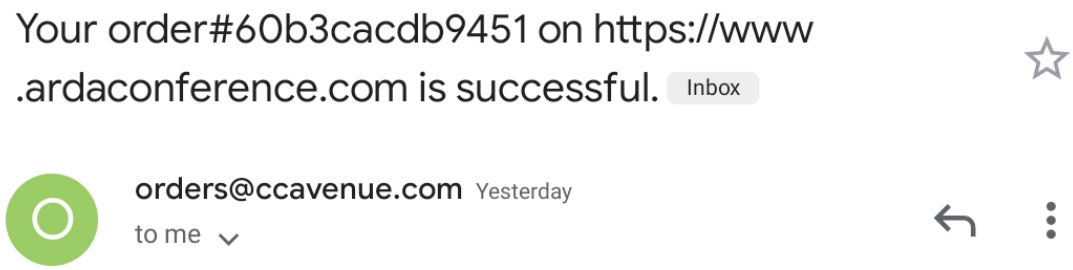

Your order#60b3cacdb9451 on https://www .ardaconference.com is successful. Inbox

orders@ccavenue.com Yesterday

to me

ARDA Conference Pvt Ltd

Dear **Sudeb Sarkar**,

Thank you for your order from https://www.ardaconference.com

For your convenience, we have included a copy of your order below. The charge will appear on your credit card / Account Statement as '**www.ardaconference.com**'

Order#	CCAvenue Reference #	Order Date
60b3cacdb9451	110172490279	30/05/2021 23:00:12

Billing Details

Customer:	Sudeb Sarkar | sarkar.sudeb@gmail.com | 8527939835
Address:	CR Park New Delhi ,Delhi ,New Delhi 110019. India
Customer IP:	27.58.235.155
Pay Mode:	Debit Card - Visa Debit Card
Bank Ref #:	360003
Instructions:	Conference&Journal

Order Amount: INR 4727.81

Net Payable: INR 4727.81

Shipping Details

Contact Person:	Sudeb Sarkar | 8527939835
Address:	CR Park New Delhi, Delhi, New Delhi 110019. India

CUSTOMER CARE
https://ardaconference.com
Email : siddth@ardaconference.com
Contact Info : 44-2080892983

Powered by CCAvenue

CONTENTS

LIST OF FIGURES

ABSTRACT

Structures which are periodic in their permittivity, and have their lattice constant lengths in the order of wavelength can show photonic bandgaps. Photonic bandgaps give information about the range of frequencies in which no modes pass through the periodic structure. In this work we explore the theory behind the occurrence of band gaps, the tools required to study photonic band gaps, the effect of geometries on bandgaps, as we examine various square lattices to examine their bandgaps, and we use one of the structures to create a photonic crystal waveguide by introducing defects.

CHAPTER 1

INTRODUCTION

In Solid State Physics, we have crystal structures which are periodic in the atomic scale. However the periodic structures being considered in this work are periodic at lengths much larger than the atomic scale. Here the periodicity of structures are at the wavelength scale. Therefore larger the wavelength, larger the size of the structures, and therefore the order of length at which the substance is periodic is also larger. This also tells us about the scalability of the periodic structures, that the same periodic structures at different sizes can be used for wavelengths of different orders of magnitude.

The mathematical basis of periodic structures can be taken from Quantum Mechanics, and particularly the Kronig Penney model. This model looks at microscopic periodic structures, and how periodic potentials, lead to electronic band gaps, that we see in substances like semiconductors. Similarly, in our case, instead, of a periodic variation in potential we look at a periodic variation in dielectric constant/refractive index, and see how that gives us photonic band gaps. And instead of the Schrodinger's equation, it is the generalized wave equation that is being solved.

In particular the periodic structures we'll be discussing in this work, are band gap materials, whose periodicity with respect to permittivity leads to the formation of photonic band gaps, which don't allow waves of certain frequencies and polarizations to pass through the given materials in certain (or all) directions.

1.1 ORGANIZATION OF THE DOCUMENT

In this document we'll firstly be explaining the origin of bandgaps, by very briefly talking about the Kronig Penney model and then starting with the Maxwell equations, deriving the generalized wave equation, and introducing Bloch waves. We'll be discussing how the variational equation gives rise to conditions that lead to the formation of a band gap.

We'll be discussing reciprocal lattices, its relation to the direct lattice and its physical interpretation, the Brillouin Zone and the Irreducible Brillouin Zone and thereafter understanding what band diagrams are and the information that we get from them.

We then do calculations required in order to get the irreducible brillouin zone for square lattices. We obtain band gap diagrams of various lattice structures and discuss the various factors that affect the characteristics of the band gaps, and as an application we'll be showing how these band diagrams can be used to design waveguides.

CHAPTER 2

THEORETICAL BACKGROUND

2.1 GENERALISED WAVE EQUATION

The Maxwell's equations for free space (no charge or current sources) are given by

$$\vec{\nabla}.\vec{D} = 0 \quad (2.1)$$

$$\vec{\nabla}.\vec{B} = 0 \quad (2.2)$$

$$\vec{\nabla} \times \vec{E} = -\frac{\partial \vec{B}}{\partial t} \quad (2.3)$$

$$\vec{\nabla} \times \vec{H} = \frac{\partial \vec{D}}{\partial t} \quad (2.4)$$

Where

$\vec{E}$ is the Electric Field Vector

$\vec{H}$ is the Magnetic Field Vector

$\vec{D}$ is the Electric Flux Vector

$\vec{B}$ is the Magnetic Flux Vector

Along with the constitutive relations

$$\vec{D} = \epsilon\vec{E} \quad (2.5)$$

$$\vec{B} = \mu\vec{H} \quad (2.6)$$

ϵ is the permittivity of the medium

μ is the permeability of the medium

Transforming the equations to the frequency domain gives us

$$\vec{\nabla}.\vec{D} = 0 \quad (2.7)$$

$$\vec{\nabla}.\vec{B} = 0 \quad (2.8)$$

$$\vec{\nabla} \times \vec{E} = -j\omega\vec{B} \quad (2.9)$$

$$\vec{\nabla} \times \vec{H} = j\omega\vec{D} \quad (2.10)$$

ω is the frequency of the wave

Putting the constitutive relations into the last two Maxwell equations (assuming the materials are non-magnetic) gives us

$$\vec{\nabla} \times \vec{E} = -j\omega\mu_0\vec{H} \quad (2.11)$$

$$\vec{\nabla} \times \vec{H} = j\omega\epsilon_0\epsilon_r\vec{E} \quad (2.12)$$

Writing $\vec{E}$ in terms of $\vec{H}$ in 2.12

$$\vec{E} = -\frac{j}{\omega\epsilon_0\epsilon_r}(\vec{\nabla} \times \overrightarrow{H}) \quad (2.13)$$

And putting 2.13 in 2.11

$$\nabla \times \left(-\frac{j}{\omega \epsilon_0 \epsilon_r} \left(\vec{\nabla} \times \vec{H} \right) \right) = -j\omega \mu_0 \vec{H} \quad 2.14$$

Gives the generalized wave equation.

$$\nabla \times \left(\frac{1}{\epsilon_r} \left(\vec{\nabla} \times \vec{H} \right) \right) = \omega^2 \mu_0 \epsilon_0 \vec{H} \quad 2.15$$

$$\nabla \times \left(\frac{1}{\epsilon_r} \left(\vec{\nabla} \times \vec{H} \right) \right) = k_0^2 \vec{H} \quad 2.16$$

Where

$$k_0^2 = \omega^2 \mu_0 \epsilon_0 \quad 2.17$$

We can see that 2.16 is in the form of an Eigenvalue problem

2.2 BLOCH WAVES

Let's understand the concept of Bloch waves.

When a plane wave is travelling through air ($n = 1$) where n is the refractive index, it travels with the velocity of light $v = c$, as $n = c/v$. However if the wave travels through a medium with greater refractive index($n > 1$), then $v < c$ because travelling through a higher refractive index medium slows the wave down.

Therefore if we compare the pattern of the wave travelling through air, and the wave travelling through a finite dielectric block for example, we'll see that in comparison to the wave travelling through air, the wave that came out of the dielectric block will be perturbed.

If instead of the aforementioned dielectric block, we had a periodic variation of the dielectric (Fig 2.1), similar to the distribution of potential wells in the Kronig-Penney model. And upon them we made incident a plane wave, the resultant wave after coming out wouldn't just be a plane wave, but would also have characteristics of the periodic medium that it is passing through.

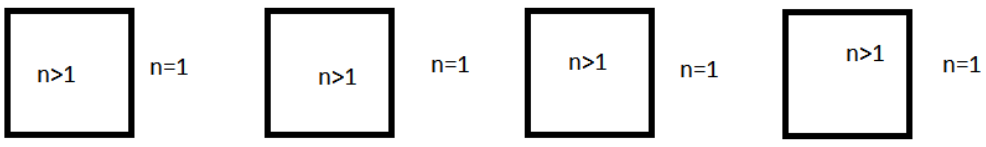

Fig. 2.1: A periodic medium in one dimension with periodically changing refractive index

More specifically, the field has the same periodicity and symmetry as that of the periodic structure that it is passing through. However the plane wave nature of the field doesn't completely change. Therefore the Bloch wave is a product of two terms

$$\vec{E}(\vec{r}) = \vec{A}(\vec{r})e^{j\vec{\beta}.\vec{r}} \quad 2.18$$

Where,
$\vec{E}(\vec{r})$ is the overall field
$\vec{A}(\vec{r})$ is the amplitude of the field which has the periodicity and symmetry characteristics of the periodic structure
$e^{j\vec{\beta}.\vec{r}}$ is the plane wave term which is the same as that of the incident wave
$\vec{\beta}$ is the wave vector which gives the direction perpendicular to the wave front of the plane wave also known as the Bloch wave vector

Therefore the plane wave term is modified by the amplitude term to give it the characteristics of the periodic structure it is passing through, that is, if

$$\epsilon\left(\vec{r} + \vec{t}\right) = \epsilon(\vec{r}) \quad 2.19$$

Where $\vec{t}$ denotes the periodicity of the permittivity then

$$A\left(\vec{r} + \vec{t}\right) = A(\vec{r}) \quad 2.20$$

2.3 ORIGIN OF THE BAND GAP

Therefore when we put our Bloch wave eq. 2.18 in the generalized wave equation eq. 2.16, what we try to do is that for each wave vector $\vec{\beta}$ we try to solve the Eigenvalue problem. And for every mode i of the field H_i we get $k_{0,i}$, the eigenvectors of eq. 2.16

Where,
H_i denotes the modes of the field being made incident upon the periodic structure
$k_{0,i}$ denotes the eigenvalues which denote the frequency of the wave from 2.17

Physically there are ∞ modes that can exist however computationally only a finite number of modes can be calculated.

According to the electromagnetic variational theorem, the lowest frequency mode, i.e., the mode with the lowest $k_{0,i}^2 = \frac{\omega^2}{c^2}$ will minimize the expression

$$U_f = \frac{\int d^3r \left|\nabla \times \vec{E}(\vec{r})\right|^2}{\int d^3r\, \epsilon(\vec{r}) \left|\vec{E}(\vec{r})\right|^2}$$

It can be seen that in order to minimize the above expression, the Electric field $\vec{E}$ of the lowest mode must be concentrated in the regions of the highest permittivity ϵ.

One of the properties of the modes is different modes must be orthogonal, which means that the field patterns of the various modes are completely different. In a one dimensional photonic crystal for example we have the following.

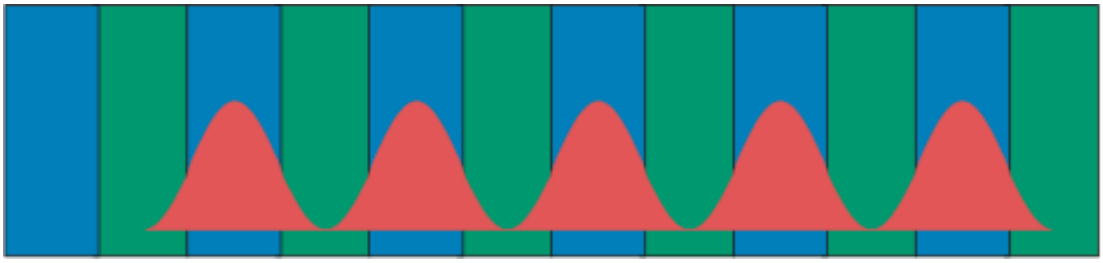

Fig. 2.2: Blue denotes higher permittivity/refractive index, and depicts the lowest frequency modes having their Electric Field energy being concentrated in the higher RI regions

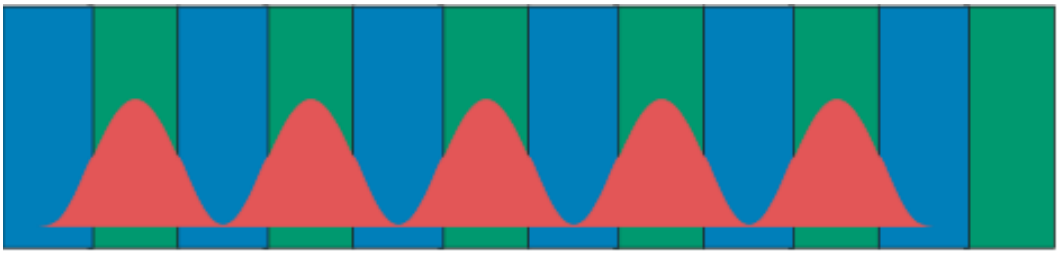

Fig. 2.3: The higher band has its Electric Field distribution orthogonal to the lower frequency mode, therefore its energy concentration is opposite of the lower frequency mode

On average the two waves experience different refractive indices (due to their energies being concentrated in different zones) and therefore the lower band on average experiences a higher refractive index and the upper band experiences a lower refractive index. However the light is moving with the same velocity and wavelength

Therefore by,

$$\omega = \frac{c_0 k}{n} = \frac{c_0}{n}\frac{2\pi}{\lambda} \qquad 2.21$$

As n is different and λ is the same therefore ω must be different which results in the bandgap.

This concept of bandgap can be extrapolated similarly to structures which are periodic in 2 and 3 dimensions to explain the existence of higher dimensional bandgaps.

2.4 RECIPROCAL LATTICE

Direct lattice vectors define the direct lattice, if we take two lattice vectors and draw a vector perpendicular to the plane formed by it, we get a reciprocal lattice vector whose magnitude is proportional to the reciprocal of the interplanar spacing of the direct lattice.

In a direct lattice the non-primitive lattice vectors are given by

$$\overrightarrow{t_{pqr}} = p\overrightarrow{t_1} + q\overrightarrow{t_2} + r\overrightarrow{t_3} \qquad 2.22$$

Where $\overrightarrow{t_1}, \overrightarrow{t_2}, \overrightarrow{t_3}$ are primitive direct lattice vectors

Each plane in the direct lattice is donated by the Miller indices(hkl), and these miller indices are related to the non-primitive reciprocal lattice vectors by

$$\overrightarrow{T_{hkl}} = h\overrightarrow{T_1} + k\overrightarrow{T_2} + l\overrightarrow{T_3} \qquad 2.23$$

Where $\overrightarrow{T_1}, \overrightarrow{T_2}, \overrightarrow{T_3}$ are primitive reciprocal lattice vectors that can be obtained from the primitive direct lattice vectors using the following formulae

$$T_1 = 2\pi \frac{\overrightarrow{t_2} \times \overrightarrow{t_3}}{\overrightarrow{t_1}.\left(\overrightarrow{t_2} \times \overrightarrow{t_3}\right)} \qquad 2.24a$$

$$T_2 = 2\pi \frac{\overrightarrow{t_3} \times \overrightarrow{t_1}}{\overrightarrow{t_1}.\left(\overrightarrow{t_2} \times \overrightarrow{t_3}\right)} \qquad 2.24b$$

$$T_3 = 2\pi \frac{\overrightarrow{t_1} \times \overrightarrow{t_2}}{\overrightarrow{t_1}.\left(\overrightarrow{t_2} \times \overrightarrow{t_3}\right)} \qquad 2.24c$$

In an analogous way the primitive direct lattice can be obtained from the reciprocal lattice vectors using the following formulae

$$t_1 = 2\pi \frac{\overrightarrow{T_2} \times \overrightarrow{T_3}}{\overrightarrow{T_1}.\left(\overrightarrow{T_2} \times \overrightarrow{T_3}\right)} \qquad 2.25a$$

$$t_2 = 2\pi \frac{\overrightarrow{T_3} \times \overrightarrow{T_1}}{\overrightarrow{T_1}.\left(\overrightarrow{T_2} \times \overrightarrow{T_3}\right)} \qquad 2.25b$$

$$t_3 = 2\pi \frac{\overrightarrow{T_1} \times \overrightarrow{T_2}}{\overrightarrow{T_1}.\left(\overrightarrow{T_2} \times \overrightarrow{T_3}\right)} \qquad 2.25c$$

Therefore each point on the reciprocal lattice vector refers to a plane in the direct lattice.

2.5 BRILLOUIN ZONE

The Wigner Seitz cell of any direct lattice is the smallest primitive unit cell for the direct lattice. It is constructed by

1) Choosing a lattice point
2) Connecting the lattice point to all nearby lattice points by lines
3) Bisecting those lines perpendicularly and joining those lines.

Smallest volume enclosed by these perpendicular lines constitute the Wigner Seitz cell of the direct lattice with primitive lattice direct vectors $\overrightarrow{t_1}, \overrightarrow{t_2}, \overrightarrow{t_3}$. In a similar way, if we were to look at the reciprocal lattice constituted by the primitive reciprocal lattice vectors $\overrightarrow{T_1}, \overrightarrow{T_2}, \overrightarrow{T_3}$ and do the same procedure that we did to create the Wigner Seitz Cell, we would get the 1st Brillouin Zone of the reciprocal lattice.

Therefore the 1st Brillouin Zone can be said to be the primitive unit cell of the reciprocal lattice.

However unit cells may not necessarily be the smallest quantity that a lattice can be reduced to. If the unit cell has symmetry, then we can divide the unit cell into smaller sections, and therefore the Brillouin Zone can also be reduced into smaller sections. These smaller sections of the Brillouin Zone which are created due to the symmetry present in the unit cell of the direct lattice is known as the irreducible Brillouin zone.

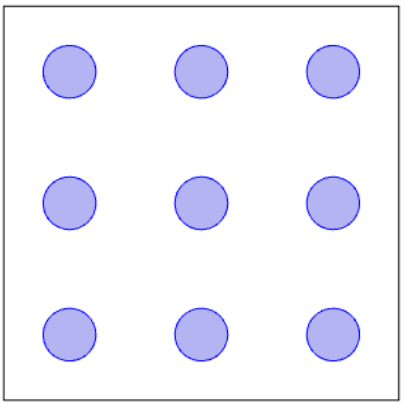

Fig. 2.4: A square lattice

For a unit square lattice in 2D we see that in order to analyse this lattice, we can just analyse the unit cell instead in order to reduce computational time. Therefore reducing this to the unit cell we get

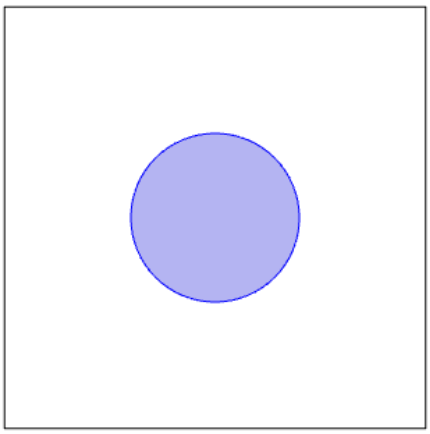

Fig. 2.5: Unit cell of square lattice in Fig 2.4

However we see that this unit cell also exhibits further symmetry i.e., it has reflection symmetry across the vertical axis, it has reflection symmetry across the horizontal axis, and it also has rotational symmetry when rotated by 90°. Therefore accounting for all

these symmetries, we get an even smaller part of the unit cell, which when repeated gives us the unit cell and therefore the whole lattice

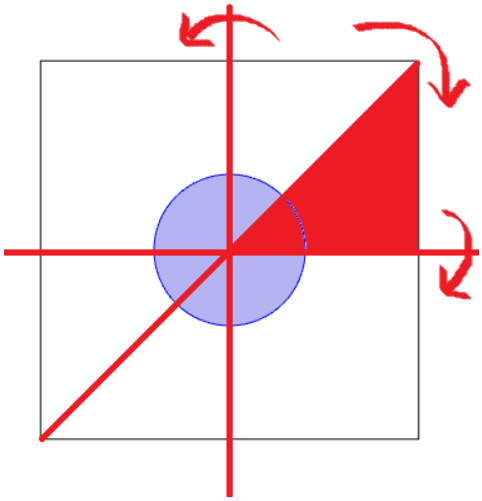

Fig. 2.6: Depicting the symmetries of the square lattice namely a)reflection symmetry along the vertical axis b) reflection symmetry along the horizontal axis c)90° rotational symmetry

Therefore this is smallest part of the direct lattice that cannot be further subdivided to give us symmetrical sub parts. Correspondingly for its reciprocal lattice which is also square we get the Irreducible Brillouin Zone (IBZ) due to the symmetry of the unit cell.

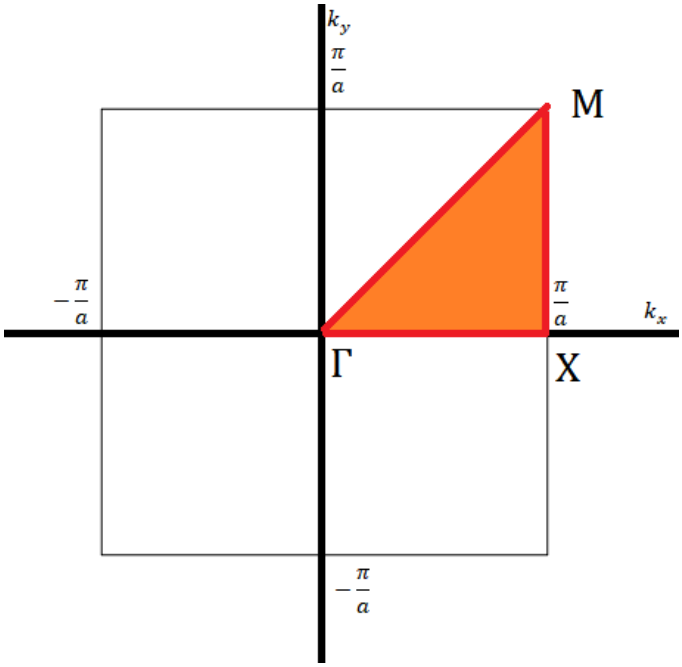

Fig. 2.7: The Brillouin Zone (square), and the Irreducible Brillouin Zone (coloured triangle) of the square lattice unit cell in Fig. 2.5

The coloured triangular portion of this reciprocal lattice is called the Irreducible Brillouin Zone (IBZ). The points Γ, X, M denote the various points of symmetry.

CHAPTER 3

METHODOLOGY

3.1 FINITE ELEMENT METHOD

The simulations have been done on COMSOL Multiphysics which works on the basis of the Finite Element Method. This method is particularly useful for solving electromagnetic problems in complex geometries which involve media with inhomogeneity in permittivity or permeability.

In order to apply FEM the following steps are required

1) The geometry, which constitutes the solution region must be divided into a number of small portions/elements by the use of a mesh.
2) Each individual element has equations derived for it
3) All the elements of the entire geometry of the solution region is assembled together
4) The resulting equations are then solved

Discretizing – When we discretize the solution region into smaller elements, we divide the whole region into what's known as the finite elements. The entire solution region is divided into various shapes manually or by software algorithms. The more the finite elements the more accurate the solution, however it also results in a higher computational cost. The solution region whether in $1D, 2D\ or\ 3D$ can be divided into a variety of shapes.

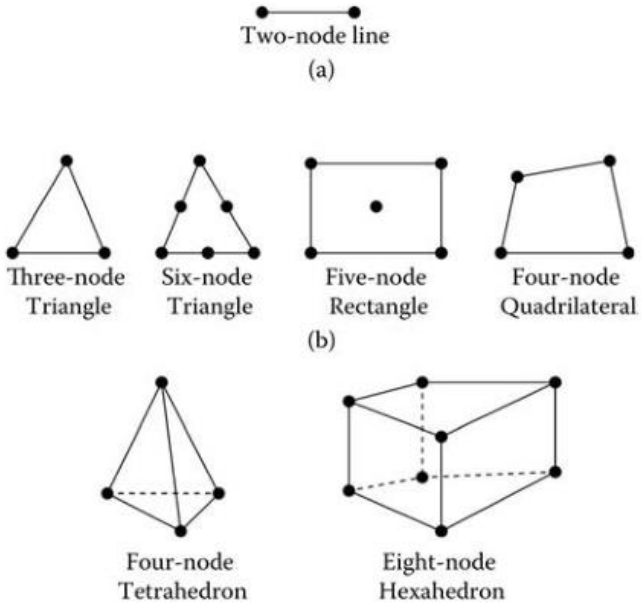

Fig. 3.1: Various meshing shapes that can be used as elements in Finite Element Method

Equation derivation for a singular element – Given the equation that needs solving we make assumptions about the approximate form of the solution for each element and we put that in matrix form. And we are able to get an equation which can give us a solution

for each point inside our element. As has been expressed before, smaller the element, the more accurate this expression will be and therefore the more accurate will be the solution at each point. We also create the element coefficient matrix which gives us the coupling between the various nodes inside of an element.

Assembling of all elements – Just like how we created a coefficient matrix for a single element, now we'll create another coefficient matrix known as the global coefficient matrix which will take into account the relation of the various nodes of different elements with each other in the solution region. Therefore the various nodes will have two kinds of numbering, a local numbering for inside the element, and a global numbering for the larger solution region. Because there are a large number of nodes which do not share a line with each other, therefore a majority of the numbers in this global coefficient matrix will be zero.

Result Computation – We thereafter iteratively compute all the approximate solutions for every single element that we have created in our geometry. We firstly find the values at the nodes and thereafter we find values on the inside by the equations that were derived for every individual element.

3.2 BAND DIAGRAMS

Band diagrams are diagrams that can denote the EM properties of a material. For each direction of the Bloch wave vector $\vec{\beta}$ we can use the eigenvalue equation 2.16 to get the eigenvalues $k_{0,i}$ for each mode H_i. Now if we take the Bloch wave vector direction along the perimeter of the Irreducible Brillouin Zone

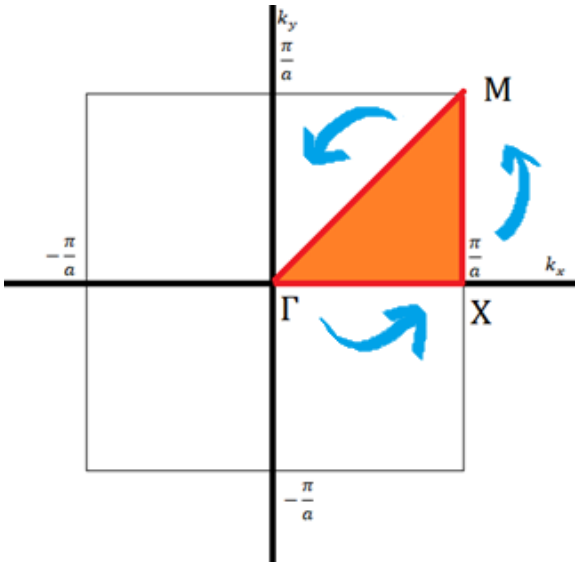

Fig. 3.2: Traversing the perimeter of the Irreducible Brillouin Zone for the square lattice

Therefore we traverse the perimeter along the path

$$M \rightarrow \Gamma \rightarrow X \rightarrow M$$

This perimeter ends up forming the x-axis of our band diagram. The y axis of the EM band diagram represents the normalized frequency. We use normalized frequency because periodic structures like these do not have any fundamental length scale, and

therefore if similar properties are required for a different orders of wavelength, they can simply be scaled up with a proportional change in the size of the side of the unit cell. Consider that the side of the unit cell is given by a, the wavelength is given by λ, and the angular frequency by ω. Therefore the y axis of a band diagram consists of the normalized quantity $\frac{a}{\lambda_0} = \frac{\omega a}{2\pi c}$. This makes the band diagram size independent and allows us to scale the results accordingly.

Therefore for a structure with a silicon rods of permittivity $\epsilon = 12.5$ and radius of rods $R = 0.2a$

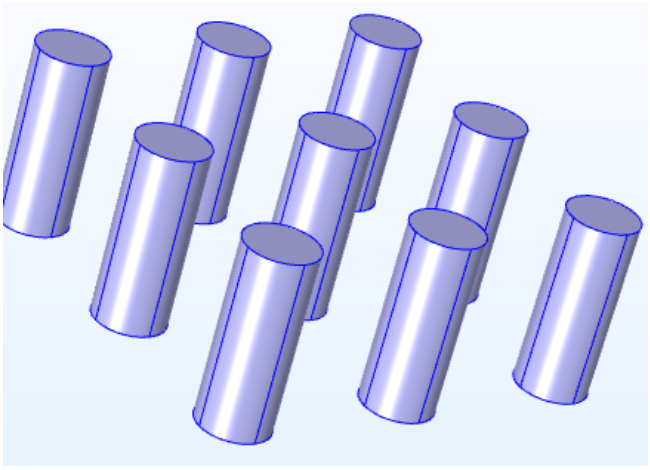

Fig. 3.3: Silicon rods embedded in air with radius of rods $R = 0.2a$

If we take this structure in the 2D domain and take only the unit cell we get the familiar square unit cell discussed above. Now we take out the band diagram for the structure by making the Bloch vector incident upon the structure vary along the perimeter of the Irreducible Brillouin Zone. Therefore our Block Wave vector β becomes a function of k_x and k_y and this is instead denoted by the points of symmetry of the lattice.

For the TM mode (i.e. the electric field vector is polarized perpendicular to the plane) we get the following band diagram

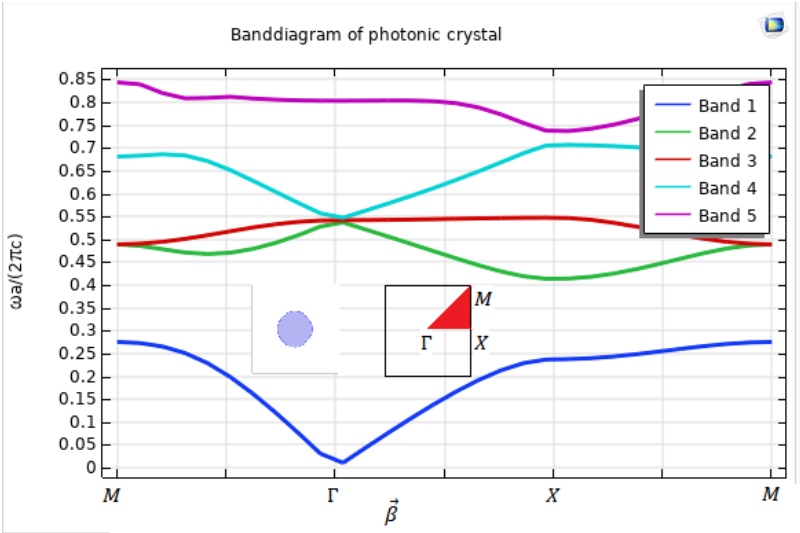

Fig. 3.4: Band diagram of silicon rods embedded in air for TM modes with radius of rods $R = 0.2a$

However for the TE mode (i.e., the electric field in polarized in the plane) we get the photonic diagram

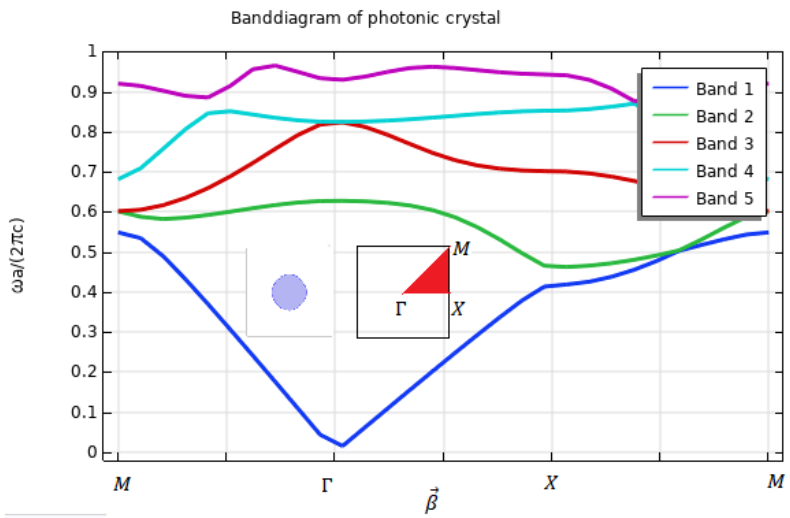

Fig. 3.5: Band diagram of silicon rods embedded in air for TE modes with radius of rods $R = 0.2a$

Therefore it can be observed that the same structure can show very different EM band diagrams for different polarizations. In our case for dielectric rods embedded in air, we see that we have a band gap for TM modes and we don't have a band gap for TE modes.

Let us consider another structure, where instead of dielectric rods, we've dielectric veins embedded in air

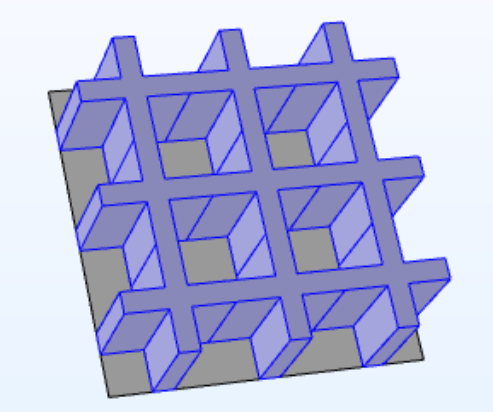

Fig. 3.6: Silicon Veins embedded in air with width of veins $W = 0.2a$

Given that this lattice has the same symmetry conditions as the one with the dielectric rods, the Irreducible Brillouin Zone will take the same shape and the unit cell will look as follows

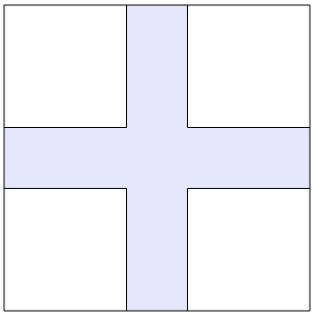

Fig. 3.7: Unit cell of lattice with Silicon Veins embedded in air with width of veins $W = 0.2a$

If on this lattice we made incident the TM mode we get the band diagram which shows no band gaps for the TM mode unlike the previous case. Here the dielectric veins have a relative permittivity of 12.5 and have a width $W = 0.2a$

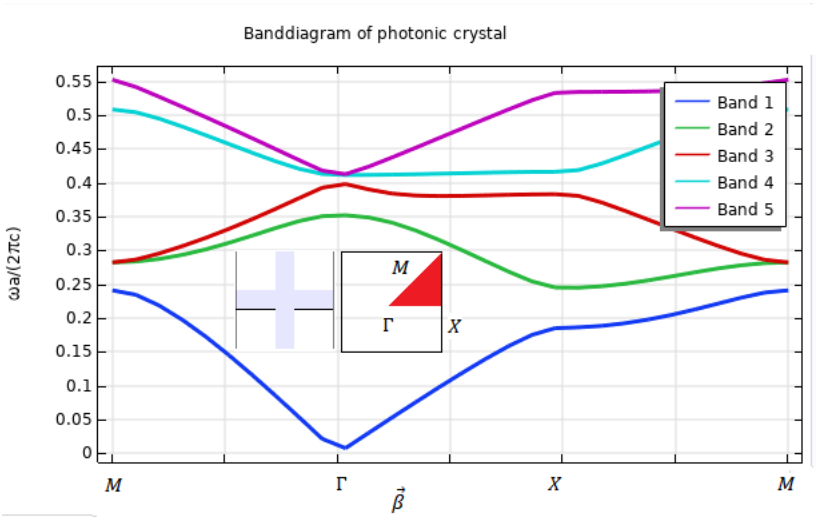

Fig. 3.8: Band diagram of silicon veins embedded in air for TM modes with vein width $W = 0.2a$

However this structure for TE modes give us a band gap.

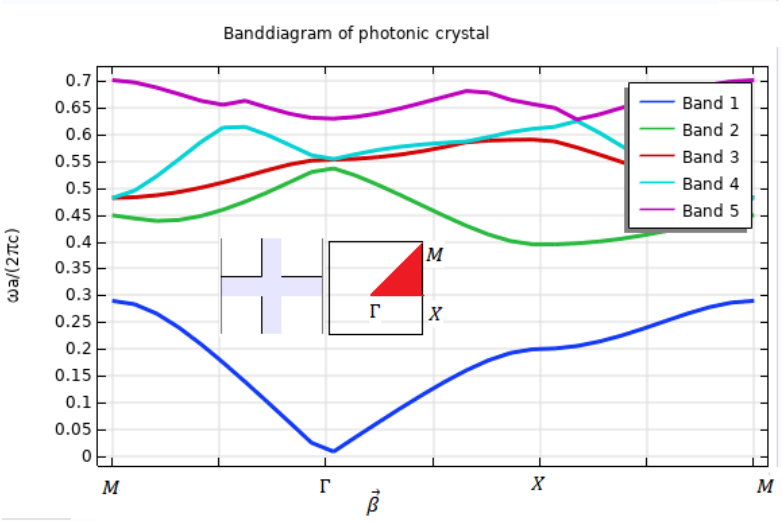

Fig. 3.9: Band diagram of silicon veins embedded in air for TE modes with width of veins $W = 0.2a$

Therefore it is apparent that geometry plays a large part in the formation of band gaps for waves of different polarizations.

Taking another structure which basically inverts the structure of dielectric rods in air to holes in a dielectric medium. Where the radius of the holes is $R = 0.2a$ and they are in a medium of permittivity $\epsilon = 12.5$ surrounded by holes of air $\epsilon = 1$

The unit lattice looks like

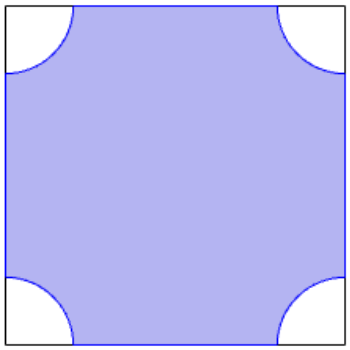

Fig. 3.10: Unit cell of lattice with air holes in Silicon with radius of holes $R = 0.2a$

Doing bandgap analysis for this lattice for both TE and TM gives us

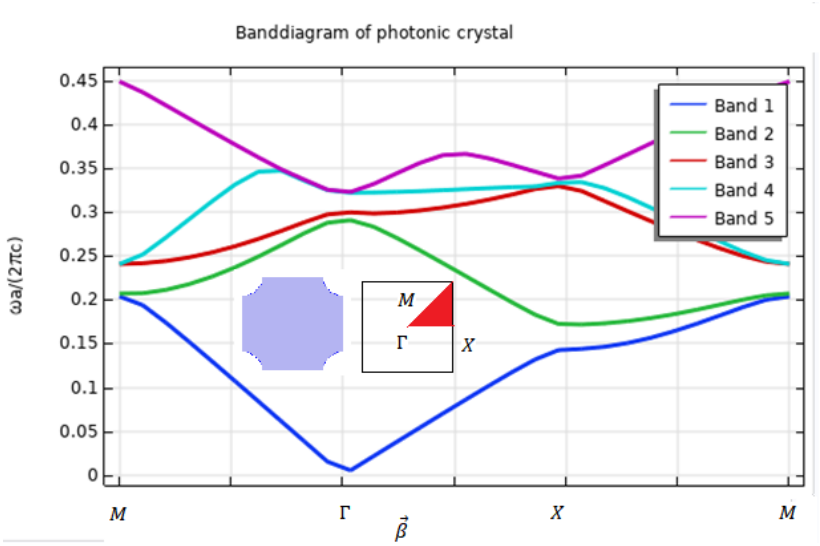

Fig. 3.11: Band diagram of air holes in silicon for TE modes with radius of holes $R = 0.2a$

For TE mode we get no band gap.

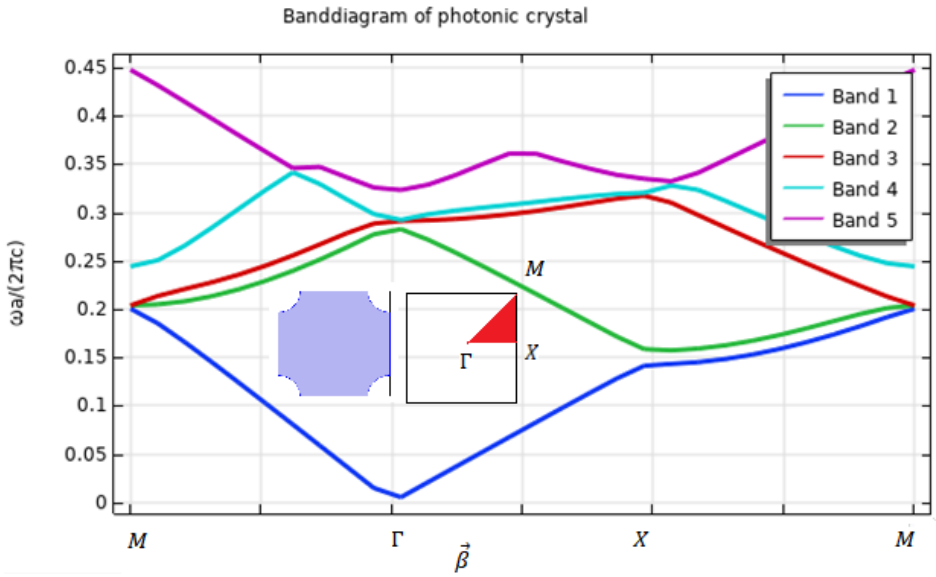

Fig. 3.12: Band diagram of air holes in silicon for TM modes with radius of holes $R = 0.2a$

For TM as well we get no band gap. If however the unit lattice is changed and instead of the hole radius being $R = 0.2a$ we change it to $R = 0.4a$ we get a lattice that looks like

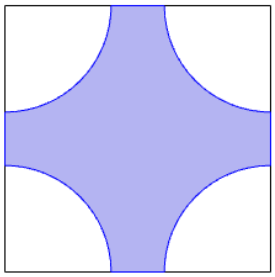

Fig. 3.13: Unit cell of lattice with air holes in Silicon with radius of holes $R = 0.4a$

For TE modes we see a rather notable and consistent band gap

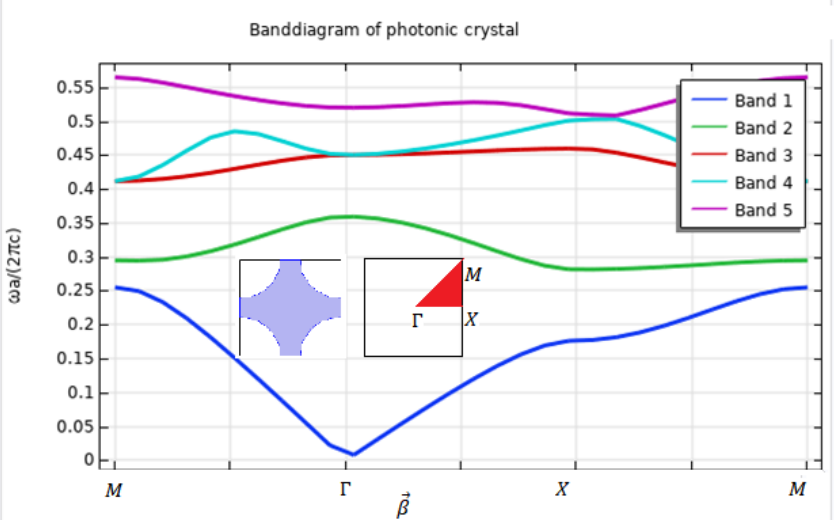

Fig. 3.14: Band diagram of air holes in silicon for TE modes with radius of holes $R = 0.4a$

For TM modes there is no bandgap to be found

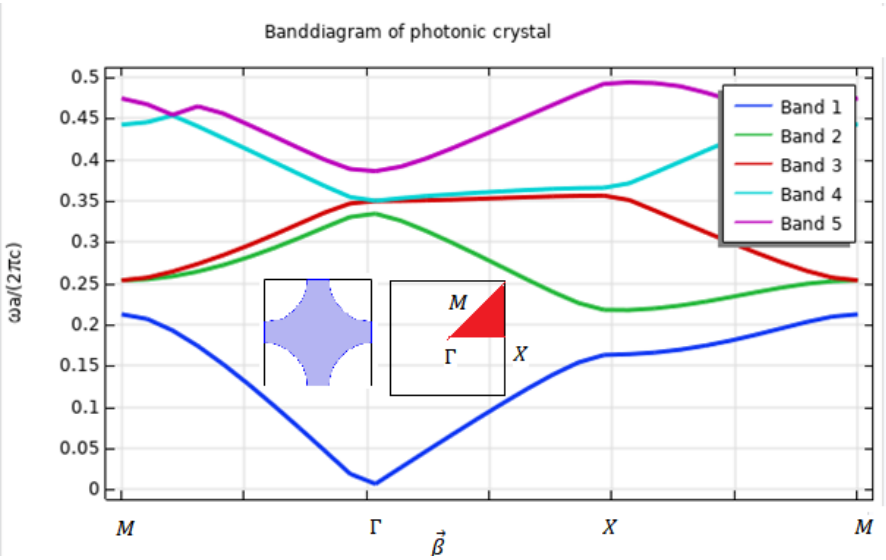

Fig. 3.15: Band diagram of air holes in silicon for TM modes with radius of holes $R = 0.4a$

If we increase the radius of the holes gradually to $R = 0.5a$.

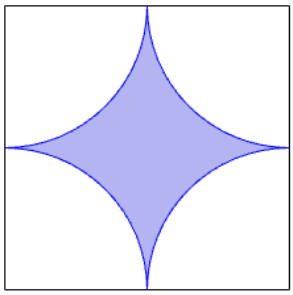

Fig. 3.16: Unit cell of lattice with air holes in Silicon with radius of holes $R = 0.5a$

For TE modes there is no longer a bandgap

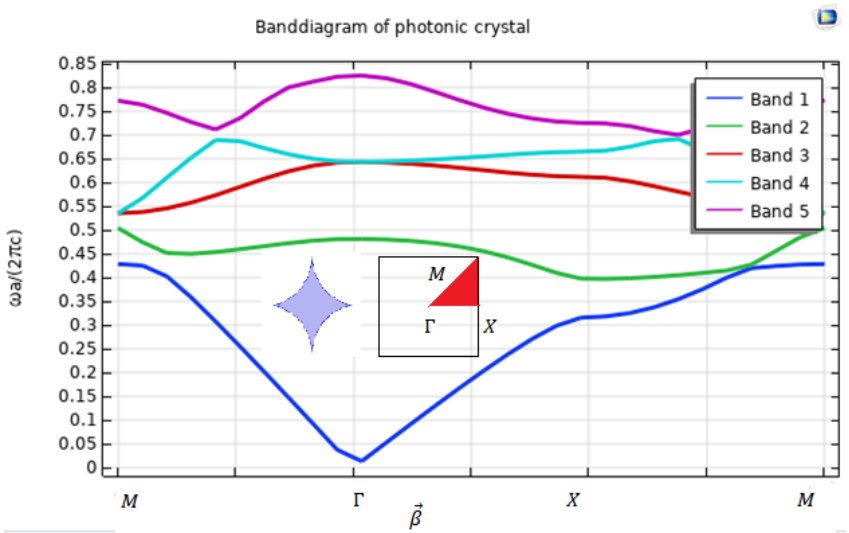

Fig. 3.17: Band diagram of air holes in silicon for TE modes with radius of holes $R = 0.5a$

However now the TM modes show a very sizeable bandgap

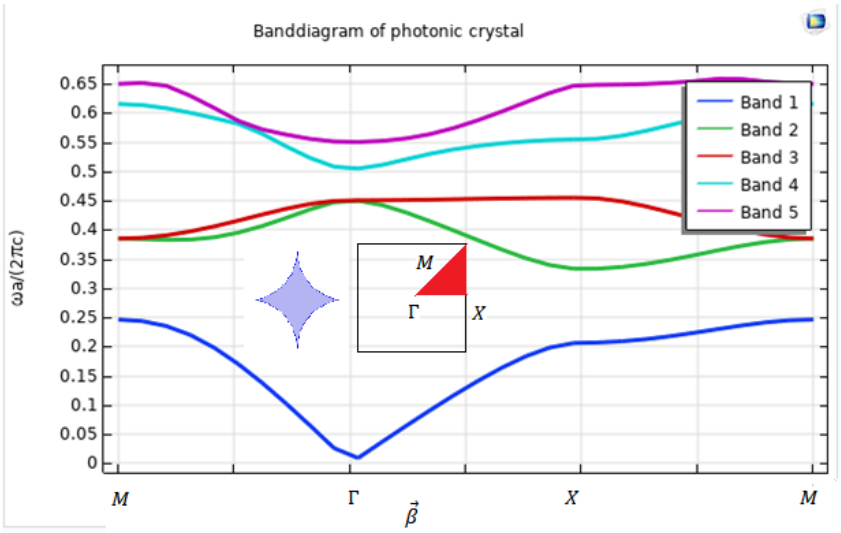

Fig. 3.18: Band diagram of air holes in silicon for TM modes with radius of holes $R = 0.5a$

Therefore even in similar lattices a change in the radius of holes can change the entire nature of the bandgaps being formed in the lattice.

CHAPTER 4

RESULTS AND DISCUSSION

We can use the band diagrams and the information of bandgaps obtained to create devices that use such periodic structures and predict their properties accordingly.

If we create a lattice using the silicon rods ($\epsilon = 12.5$) embedded in air ($\epsilon = 1$) then we can create a waveguide by introducing defects in the lattice. However unlike traditional waveguides, this waveguide can be made smaller to any extent and can be configured for light of any wavelength.

We consider a lattice whose side is $a = 1\mu m$ and the radius of the silicon rods is $R = 0.2a$. Instead of having a continuous lattice however we introduce a defect by removing an entire row of silicon rods. The lattice therefore looks like this

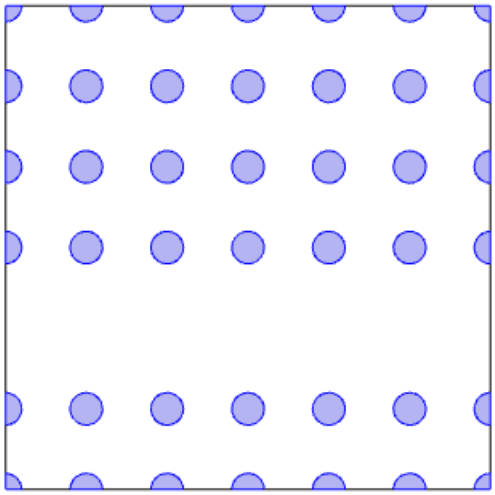

Fig. 4.1: Photonic crystal waveguide with Silicon rods $\epsilon = 12.5$ $R = 0.2a$ embedded in air

From the bandgap diagram (Fig. 3.4) we see that we have a bandgap from approximately

$$0.3 < \frac{a}{\lambda_0} = \frac{\omega a}{2\pi c} < 0.4$$

Therefore from this we get that this lattice will have a TM bandgap from approximately $2.5\mu m$ to $3.33\mu m$. On doing a wavelength analysis from $2\mu m$ to $4\mu m$ it can be seen that this wave polarized perpendicular to the plane of the lattice from $2\mu m$ to $2.2\mu m$ we don't see the wave passing through

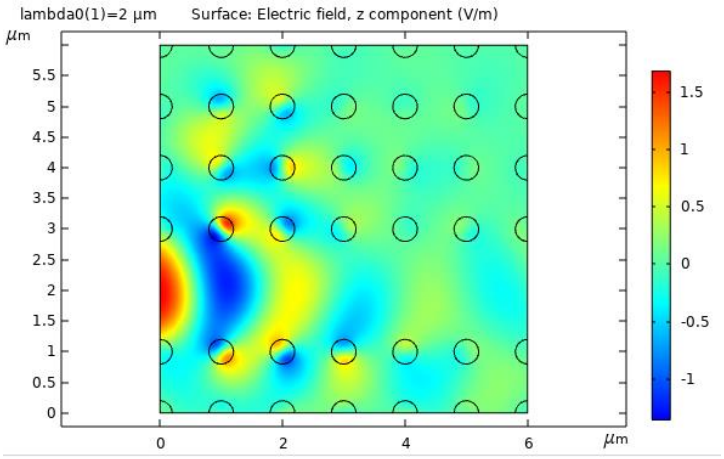

Fig. 4.2: Wave patterns of $2\mu m$ wavelength in the Photonic Crystal

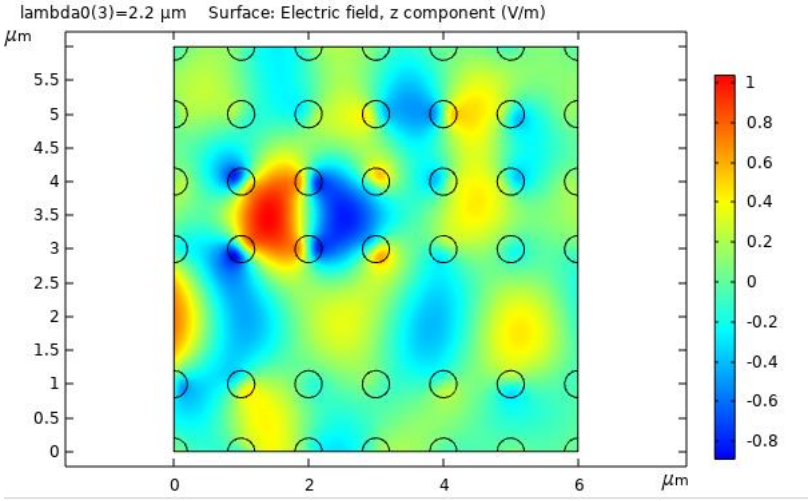

Fig. 4.3: Wave patterns of $2.2\mu m$ wavelength in the Photonic Crystal

However at $2.3\mu m$ we see a distorted waveform followed by waveguiding action from $\lambda = 2.5\mu m$ to $\lambda = 3.2\mu m$

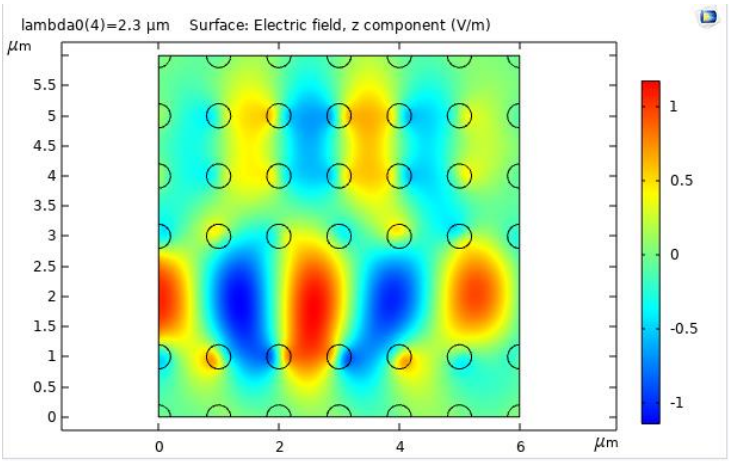

Fig. 4.4: Wave patterns of $2.3\mu m$ wavelength in the Photonic Crystal

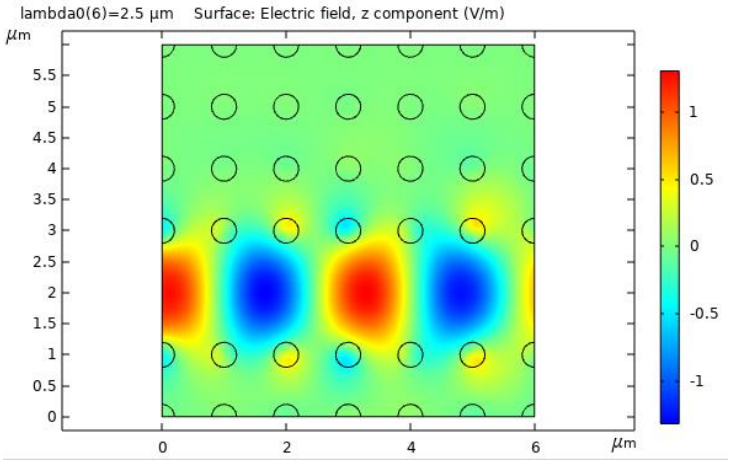

Fig. 4.5: Wave patterns of 2.5μm wavelength in the Photonic Crystal

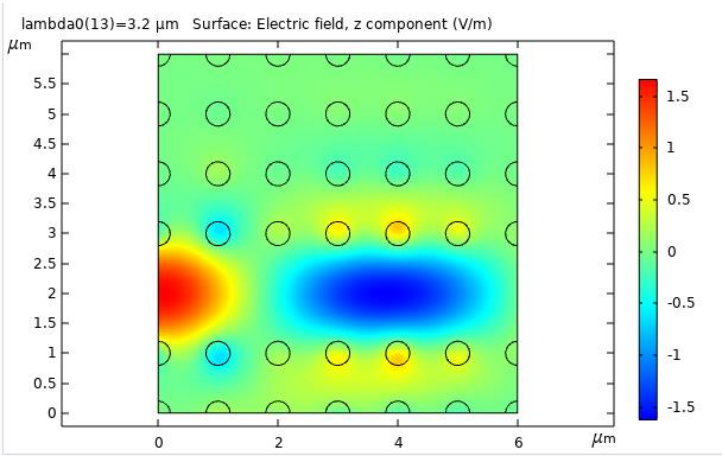

Fig. 4.6: Wave patterns of 3.2μm wavelength in the Photonic Crystal

And thereafter from 3.3μm to 4μm doesn't show any waveguiding action again. Therefore through the analysis of band diagrams of various unit cells, we can predict its electromagnetic properties which can then be used to make devices like waveguides amongst others. We also looked at the various factors which affect the bandgap including the geometry of the structure, and the polarization of the field.

REFERENCES

[1] J.D. Joannopoulos, S.G. Johnson, J.N. Winn and R.D. Meade, Photonic Crystals – Molding the Flow of Light, Second Edition, Princeton University Press (2008)
[2] X. Huang, Y. Lai, Z. H. Hang, H. Zheng, & C.T. Chan, "Dirac cones induced by accidental degeneracy in photonic crystals and zero-refractive-index materials". Nature Materials, 10(8), 582–586, May 2011.
[3] N. Shankhwar, Y. Kalra, Q. Li, R.K. Sinha, "Zero-index metamaterial based all dielectric nanoantenna" AIP Advances 9, 035115 (2019)
[4] M. N. O. Sadiku, Numerical Techniques in Electromangetics with MATLAB, Third Edition, CRC Press, 2009
[5] C. Kittel, Introduction to Solid State Physics, Eighth Edition, Wiley India Pvt. Ltd, 2019
[6] R.K. Puri, V.K. Babbar, Solid State Physics, S Chand Publishing, 2016
[7] B. E. A. Saleh, M. C. Teich, Fundamentals of Photonics, Third Edition, John Wiley & Sons, 2019

Effect of geometries on photonic bandgaps

[1]Sudeb Sarkar
[1] Department of Applied Physics, Delhi Technological University, Bawana Road, Delhi 110042, India.
[1]sarkar.sudeb@gmail.com

Abstract*— Structures which are periodic in their permittivity, and have their lattice constant lengths in the order of wavelength can show photonic bandgaps. Photonic bandgaps give information about the range of frequencies in which no modes pass through the periodic structure. In this work we explore the effect of geometries on bandgaps, as we examine various square lattices to examine their bandgaps.

Index Terms—*Bandgaps, Irreducible Brillouin Zone, Periodic Structures, Photonic Crystals*

I. INTRODUCTION

In solid state physics, the scale of periodicity is in the range of atomic lengths. The periodic structures being discussed here are in the range of wavelengths. Therefore for large waves like radiowaves, the periodicity of the structures can be visible to the eye. Periodic structures of this kind are scalable in length [1], therefore it is the geometries and the relative length of the components with respect to the lattice constant that have the most importance along with the materials used.

II. ORIGIN OF BANDGAPS

If a plane wave is incident upon a structure whose permittivity is periodic, the waves inside of the structure take the form of Bloch waves which are given by

$$\vec{E}(\vec{r}) = \vec{A}(\vec{r})e^{j\vec{\beta}.\vec{r}} \quad (1)$$

The generalized wave equation for an inhomogeneous medium is given by

$$\nabla \times \left(\frac{1}{\epsilon_r}(\vec{\nabla} \times \vec{H})\right) = k_0^2 \vec{H} \quad (2)$$

Where $k_0^2 = \omega^2 \mu_0 \epsilon_0$, $\vec{\beta}$ is the Bloch wave vector. Without simplification this equation doesn't have a solution and therefore we solve this equation as an eigenvalue problem which gives the various values of $k_{0,i} = \frac{\omega n}{c}$ and therefore gives information about the frequencies of each mode H_i. The solution of the above eigenvalue problem for each Bloch wave vector $\vec{\beta}$ on the perimeter of the Irreducible Brillouin Zone gives us the band diagram of a crystal.

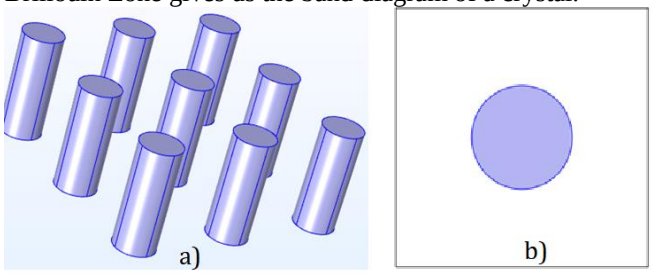

Fig. 1a) Silicon rods ($\epsilon = 12.5$) embedded in air
Fig. 1b) Unit Cell of the same lattice

III. SQUARE LATTICES

As seen in Fig 1. the square lattice has symmetry in that it remains the same through vertical reflection, horizontal reflection and rotation by 90°. Therefore the Irreducible Brillouin Zone (IBZ) of each square lattice which has the same symmetry can be given by Fig 2. Where Γ, X, M are the points of symmetry of the lattice. The reason why band diagrams are drawn on the perimeter of the IBZ and not throughout the unit lattice is because almost all the band extremes can be observed in this region and also because it saves computational time. However the information that can be derived from the entire lattice is more complete and gives us more information not available via band gap diagrams.

IV. METHODOLOGY

FEM based COMSOL multiphysics has been used in order to solve (2) for the required lattices. For a lattice that is depicted in Fig 1. with silicon rods ($\epsilon = 12.5$) [2], [3] embedded in air, we find that for an electric field that is polarized perpendicular to the plane i.e. TM modes, we get a band gap in all directions from approximately $\frac{\omega a}{2\pi c} = 0.3$ to 0.4. However for electric field that is polarized in the plane i.e. TE modes we do not have a bandgap as can be seen in Fig. 3a) and Fig. 3b) However further examination by varying aspects of the geometry changes the nature of the bandgaps.

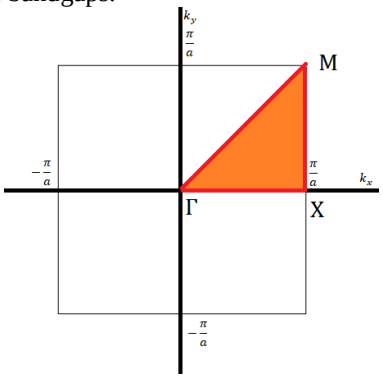

Fig. 2 The Irreducible Brillouin Zone of a square lattice which has reflection symmetry along two axes, and 90° rotational symmetry

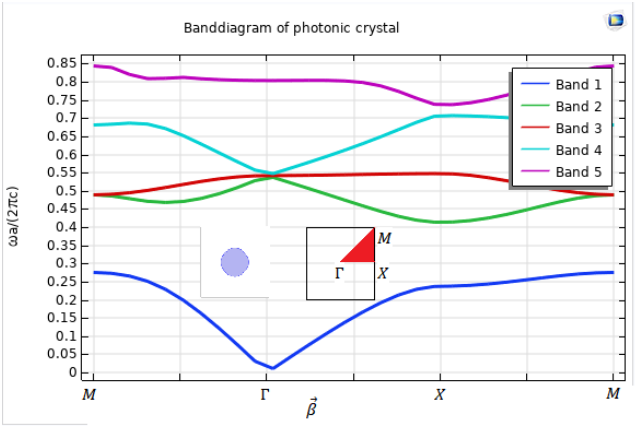

Fig. 3a) Photonic Band gap diagram for TM modes in a lattice of silicon rods embedded in air with radius of rods $R = 0.2a$, where a is the lattice constant

As the radius of the silicon rods are increased from $R = 0.2a$ to $R = 0.5a$ we see that with each increase in radius the band gap for TM modes decreases. A very narrow gap is observed for $R = 0.4a$ and thereafter at $R = 0.5a$ there is no bandgap. The TE mode bandgap diagram also does not change in nature, and we do not witness any bandgaps in this structure. Instead of dielectric rods, we now examine a structure where we have dielectric veins instead of dielectric rods of silicon ($\epsilon = 12.5$)embedded in air (Fig 4)

On calculating the bandgap diagram of this structure it was observed that for TE modes a bandgap is observed in all directions from approximately $\frac{\omega a}{2\pi c} = 0.3$ to 0.39. (Fig.5) However no bandgap was observed for TM modes. On increasing the width of the veins from $W = 0.2a$ it was observed that the bandgap for TE modes decreased continuously until at $W = 0.5a$ when the bandgap was no longer present. For TM modes the increased width also didn't bring too many changes as the lack of bandgap persisted even with the increase in width of the silicon veins.

We will now examine another lattice which is almost the inverse of the lattice depicted in Fig 1a) and Fig 1b). Instead of rods of silicon being embedded in air, we will have holes of air in a silicon lattice. Therefore we will have holes of radius $R = 0.2a$ inside a silicon lattice which will constitute our unit cell. On analysing this structure with these specifications we see that we do not get a bandgap for TE or TM polarizations. However on changing the radius of holes from $R = 0.2a$ to $R = 0.4a$ we see a difference (Fig. 6)

It can be seen that now there is a consistent bandgap for TE polarization from $\frac{\omega a}{2\pi c} = 0.25$ to 0.29 (Fig. 7)

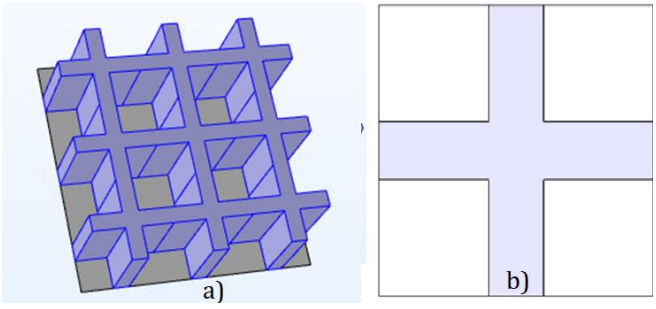

Fig. 4a) Silicon veins $\epsilon = 12.5$ in air with width $W = 0.2a$

Fig. 4b) Unit cell of the lattice

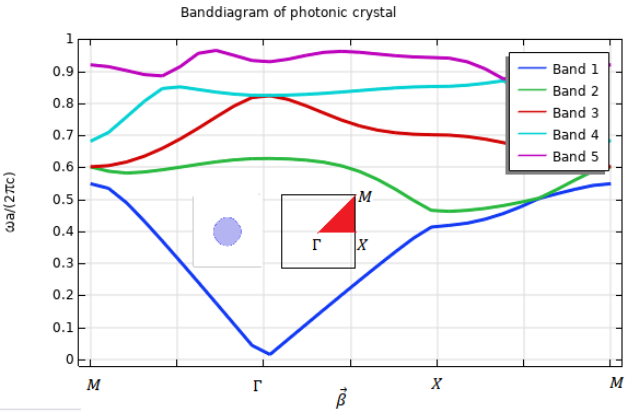

Fig. 3b) Photonic Band gap diagram for TM modes in a lattice of silicon rods embedded in air with radius of rods $R = 0.2a$, where a is the lattice constant

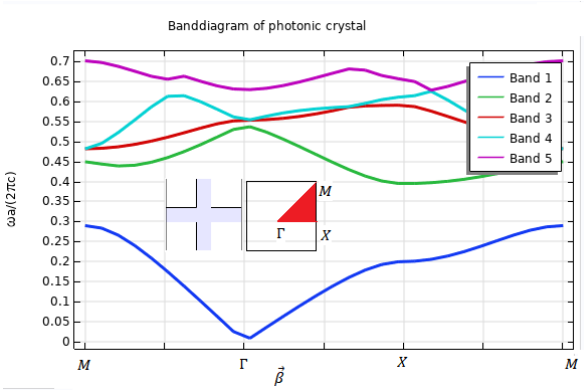

Fig. 5 Photonic Band gap diagram for TE modes in a lattice of silicon veins embedded in air with width of the veins $W = 0.2a$

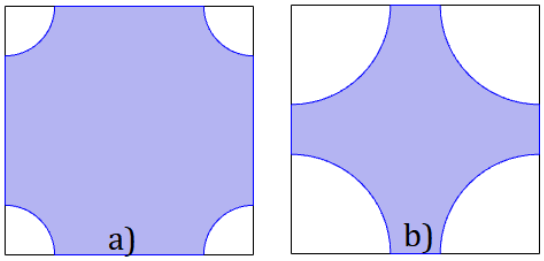

Fig. 6 Unit lattice of periodic structure of silicon with holes in it

Fig. 6a) Radius of holes $R = 0.2a$

Fig. 6b) Radius of holes $R = 0.4a$

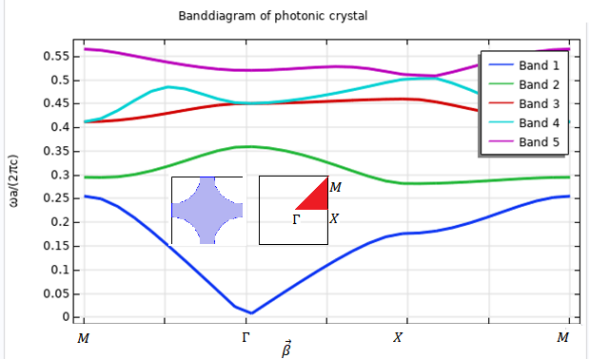

Fig. 7) Photonic Band gap diagram for TE modes in a lattice of silicon with holes of radius $R = 0.4a$

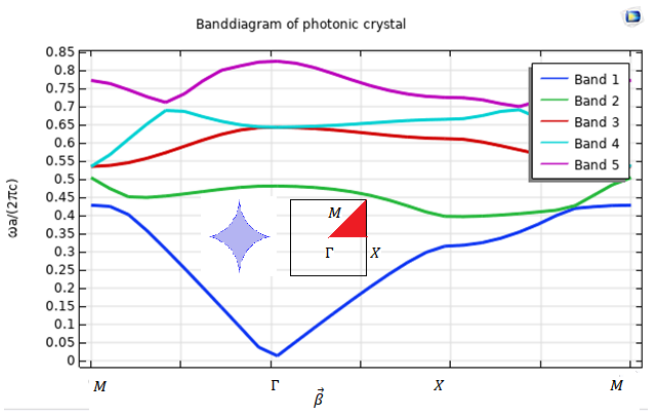

Fig 8a) Photonic Band gap diagram for TE modes in a lattice of silicon with holes of radius $R = 0.5a$. Unlike Fig. 7 there is no longer a bandgap

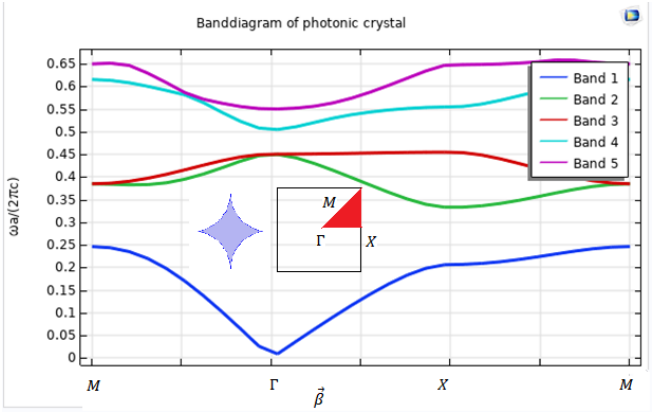

Fig 8b) Photonic Band gap diagram for TM modes in a lattice of silicon with holes of radius $R = 0.5a$. Earlier there was no bandgap for TM modes, however at $R = 0.5a$ we find a wide band gap

On further increasing the radius of the air holes from $R = 0.4a$ to $R = 0.5a$ we see that the nature of the crystal completely changes. Whereas earlier there was a narrow but consistent bandgap for TE modes, now we have a wide bandgap for TM modes with the TE mode bandgap no longer existent.

CONCLUSION

Through this study we've aimed to quantify the changes that take place in the bandgap structure of square 2D lattices, when we change its geometry. We firstly observed that dielectric rods (of higher permittivity) embedded in air (of lower permittivity) gives a bandgap for TM modes. However as the radius of the rods are increased, the bandgap seized to exist. Similarly, when instead of dielectric rods we had dielectric veins in air we got a decent bandgap for TE modes, which also seized to exist as we increased the width of the veins. In the case of air holes in the dielectric, the increasing radius of holes fundamentally changed the nature of the crystal more than once. At lower radii we didn't have band gaps for TE or TM polarizations. At higher radii we got a bandgap for TE modes. However at even higher radii this bandgap seized to exist and we instead got a wide bandgap for TM modes.

REFERENCES

[1] J.D. Joannopoulos, S.G. Johnson, J.N. Winn and R.D. Meade, Photonic Crystals – Molding the Flow of Light, Princeton University Press, 2008

[2] X. Huang, Y. Lai, Z. H. Hang, H. Zheng, & C.T. Chan, "Dirac cones induced by accidental degeneracy in photonic crystals and zero-refractive-index materials". Nature Materials, 10(8), 582–586, May 2011.

[3] N. Shankhwar, Y. Kalra, Q. Li, R.K. Sinha, "Zero-index metamaterial based alldielectric nanoantenna" AIP Advances 9, 035115 (2019)

[4] M. N. O. Sadiku, Numerical Techniques in Electromangetics with MATLAB, CRC Press, 2009